



ELSEVIER

15 July 2000

OPTICS
COMMUNICATIONS

Optics Communications 181 (2000) 361–367

www.elsevier.com/locate/optcom

Diode-pumped spatially dispersed broadband Cr:LiSGAF and Cr:LiSAF c.w. laser sources applied to short-coherence photorefractive holography

D. Parsons-Karavassilis^{*}, Y. Gu, Z. Ansari, P.M.W. French, J.R. Taylor

Femtosecond Optics Group, Department of Physics, Imperial College of Science and Technology, Prince Consort Road, London SW7 2BZ, UK

Received 23 March 2000; accepted 16 May 2000

Abstract

We demonstrate a novel high power broadband laser source for low coherence interferometry that is based on a simple three mirror diode-pumped c.w. Cr³⁺ laser. The cavity design utilises a single intracavity prism to spatially disperse the oscillating laser mode within the pumped region of the laser crystal in order to counteract spectral gain narrowing. We demonstrate continuous wave spatially coherent output beams with spectral widths as wide as 37 nm, which are tunable across the gain linewidth of the laser. Using a single 100 μm stripe width 670 nm diode pump laser we obtained output powers up to 105 mW for incident pump powers of 410 mW. We demonstrate the application of this source (adjusted for a 13 nm bandwidth output) to 3-D imaging through a diffuse medium using photorefractive holography. © 2000 Elsevier Science B.V. All rights reserved.

PACS: 42.55.Xi; 42.55.Rz; 42.60.Da; 42.62.Be

Keywords: Diode-pumped; Solid state; Broadband; Continuous wave; Imaging

1. Introduction

Low coherence interferometry for 3-D imaging, particularly through turbid media, has become an important application of ultrafast lasers. Optical coherence tomography [1] and whole-field coherence gated imaging, e.g. [2,3], are two such applications that exploit the broad spectral width of ultrashort pulses, rather than their temporal properties. An important attribute of ultrafast lasers for this applica-

tion is that they provide broadband radiation with high average power. Furthermore they also deliver a spatially coherent output beam that may be efficiently coupled into single mode optical fibres. The relative complexity and cost of mode-locked lasers, however, makes them undesirable for many practical applications. Superluminescent diodes [1] and optical fibre ASE sources [4] have been demonstrated as alternative sources of broadband, spatially coherent radiation. The former are particularly simple and cheap but their output powers and spectral widths are too low for many applications. Fibre ASE sources are currently limited in their spectral coverage and,

^{*} Corresponding author. Tel.: +44-20-7594-7784; fax: +44-20-7594-7782; e-mail: d.parsons-karav@ic.ac.uk

given their relatively high cost and typically narrower linewidths, do not usually compete with ultrafast lasers. Another approach is to synthesize a short coherence length light source by rapidly tuning a laser across its gain bandwidth, as has been demonstrated using a swept-frequency dye laser for holographic imaging [5]. This approach, however, can suffer from the complexity of an active intracavity tuning element and usually results in a relatively long image acquisition time. The ideal source would simultaneously provide high power spatially coherent radiation across the desired spectral range. We note that a Light Emitting Diode (LED) can provide 100's mW average power with spectral widths exceeding 50 nm, but these are spatially incoherent sources and so are only suitable for whole field coherent imaging techniques such as heterodyne detection [6] and photorefractive holography [7]. OCT and related techniques would benefit from a simple approach to a high average power broadband spatially coherent source that avoids the complexity of mode-locked lasers, but is still applicable to any laser medium, preferably in a diode-pumped configuration.

We present what is, to the best of our knowledge, the first tunable, diode-pumped, solid-state, c.w., broadband laser source. By exploiting spatial dispersion of the laser spectrum within the diode-pumped gain medium, we demonstrate an approach to a low-cost spectrally broadened high brightness (diffraction-limited) source that is readily scaleable to higher powers and exhibits the benefits of a solid-state laser that can utilize high power broad-stripe pump diodes while avoiding the problems associated with mode-locking such a system.

2. Intracavity spatial dispersion

The technique of spatially dispersing the beam inside the gain medium of a laser in order to counteract the effect of gain narrowing was first proposed and demonstrated in 1989 in a dye-laser [8] and then in a dye amplifier [9]. It was later applied to a Nd:YAG laser in order to sustain multi wavelength operation [10,11] and more recently applied to a Ti:Sapphire laser exploiting the large fluorescence bandwidth of this vibronic medium and ultrabroadband pulsed operation was obtained [12]. The con-

cept has also been applied to a Ti:Sapphire regenerative amplifier [13] to reduce the impact of gain narrowing. Other lasers comprising intracrystal spatial dispersion include designs for compact mode-locked lasers where it arose as an incidental property of the cavity [14], or where it was a consequence of pursuing less complex and more compact dispersion-compensated oscillators [15,16]. We note that in these mode-locked lasers the intracrystal spatial dispersion was considered a bandwidth *limiting* factor.

In this paper we describe a 3-mirror spatially dispersed cavity using either Cr:LiSAF or Cr:LiSGAF plane-Brewster cut laser crystals. Our cavity design spatially disperses the laser mode in the horizontal plane, resulting in a flattened elliptical gain region. This geometry is suitable for diode pumping since the typical output beam from a broad stripe diode or diode array results in a similarly orientated elliptical pump volume if the diode is aligned with its widest facet dimension in the plane of the cavity.

3. Experimental set-up

Fig. 1 shows the layout of the 55 cm long laser cavity. The diode beam shaping optics L1, L2 and L3 collimate and expand the beam in the horizontal axis. This pump beam is then focused into the rod, by L4, through the plane face of the crystal. This degree of focusing may be varied to optimize the degree of ellipticity in the pump region with respect to the spatially dispersed laser mode.

The main difference between a spatially dispersed spectrally broadened laser and a conventional three-mirror cavity prism-tuned laser is the position of the spectrally dispersive element from the folding mirror. This is set at a distance determined by the focal length of the particular folding mirror being employed and the angular dispersion of both the prism itself and the Brewster angle-cut rod. The degree of gain competition between neighbouring monochromatic spectral beam components (beamlets) in the pumped region of the gain medium is dependent on the degree of spatial separation between them [8]. This in turn is determined by the spot size of each monochromatic beamlet (determined by the choice of focal length of the folding mirror and the cavity length) and the degree of spatial dispersion. In our

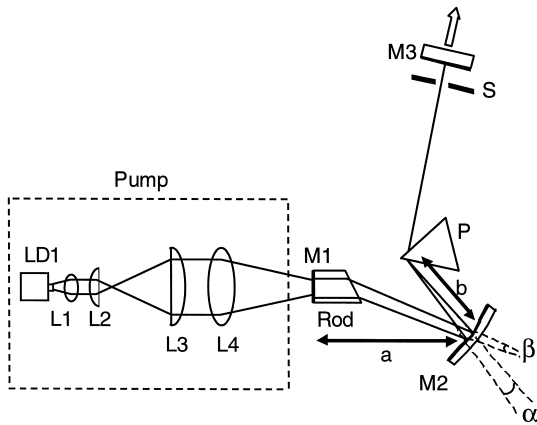


Fig. 1. Schematic of diode-pumped, three mirror spatially dispersed laser. LD1, 100- μm stripe diode at 670 nm (500 mW); L1, 4.5-mm focal length aspheric lens; L2, 6.4-mm focal length cylindrical lens; L3, 100-mm focal length cylindrical lens; L4, 50-mm focal length spherical lens; M1, end-coated high reflector mirror (HT@ \sim 670 nm and HR@ \sim 830 nm); M2, 37.5-mm focal length folding mirror; P, quartz prism; S, adjustable slit; M3, 0.5% plane output coupler.

design, the distance of the rod from the folding mirror, a , is determined by optimizing the focusing for a monochromatic beam into the rod so that it creates an appropriate beam waist at the plane mirror in the pump focus. The distance of the prism to the folding mirror, b , is set following two requirements: to have all wavelength components collinear in the long arm, and to match the spatial dispersion due to the crystal–air interface at the rod, given that all ‘monochromatic’ beams in the rod are parallel to each other and perpendicular to the mirror M1.

The angle between two single beamlets at two different wavelengths on passing through the prism (given that they were initially collinear in the long arm) is shown in Fig. 1 as α . This angle is easily calculated from the geometry of a prism and the dispersion of the material. On reflection at mirror M2, they must have a relative angle equal to β , the angle between two parallel beams at the same distinct wavelengths (initially both perpendicular to M1) that would be acquired on exiting the rod, which is simply given by Snell’s Law for refraction at an interface and is dependent on the dispersion of the rod material. The position of the prism, P , can therefore be set, using the simple mirror formula:

$$(1/\text{object}_{\text{dist}}) + (1/\text{image}_{\text{dist}}) = -(1/f)$$

The distance b becomes equal to $f(1 - \beta/\alpha)$. The degree of spatial separation in the rod between these two distinct wavelengths is then determined by the distance of the rod’s Brewster face from M2, which is in turn determined by the distance a and the length of the particular rod. Suitable positioning of the prism and adjustment of the slit S , ensures that light not dispersed in the rod, but dispersed in the long arm of the cavity experiences higher loss than light that is spatially dispersed in the rod.

In practice the accuracy required for the prism alignment was not critical and we observed broadened spectra for up to 20% deviation in b away from the optimum prism location. Beyond this point the prism simply acted as a tuning element in the cavity of an essentially monochromatic laser. With the prism at the appropriate position, a suitable narrowing of the slit resulted in broadband c.w. laser operation with a spatially coherent (i.e. non-dispersed) output beam at M3. We note that this combination of prism and Brewster angle-cut rod ensures that longer wavelengths experience a longer optical path length in the cavity, resulting in negative GVD [15]. This negative group velocity dispersion is small, however, compared to the material dispersion in the cavity.

4. Results

The precise form of the output signal was a sensitive function of the cavity mode adjustment, the pump beam and their relative position. In general, it was observed that the broader the spectral profile, the more modulated it became. Fig. 2 shows typical broadband spectra from our spatially dispersed 3-mirror cavity laser with different prism and folding mirror alignments. In general we observed no significant difference when using the Cr:LiSGAF or Cr:LiSAF laser crystals. Both crystals were nominally 3% doped (from VLOC). All spectra were acquired with 410 mW incident pump power from a single 100 μm stripe laser diode operating at 670 nm.

The cause of this spectral modulation was investigated. The modulation depth was observed to increase as the pump power density decreased, suggesting that a more powerful pump diode would

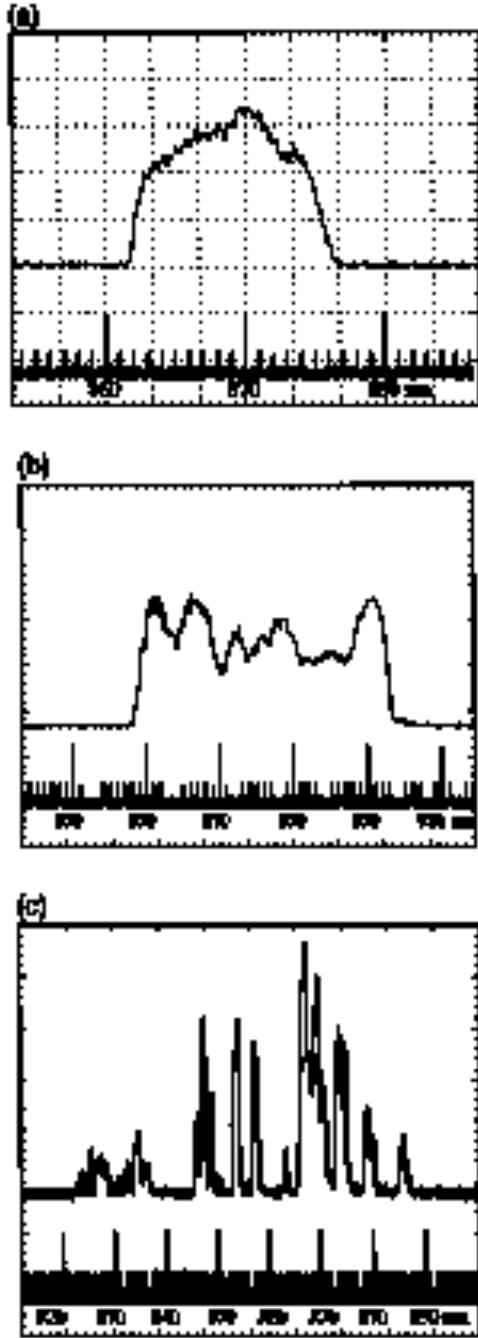


Fig. 2. Spectra of output beam from broadband c.w. laser with (a) ~ 12 nm linewidth with 53 mW (b) ~ 37 nm linewidth with 56 mW output power (c) ~ 65 nm with 39 mW output power (55% of available cavity bandwidth, determined by tuning a normal 3-mirror cavity using the same components).

result in smoother broader spectra. We speculated that, even though the elliptical pump beam was well matched to the elliptical shape of the dispersed laser beam in the crystal, spatial structure on the diode pump beam might cause the irregularities in the resulting spectrum. The intensity profile of the focused diode beam parallel to the diode stripe, observed in the plane of incidence of the cavity using a CCD camera, displayed a clearly visible mode structure, the physical spacing of the peaks in this pump beam profile when focused into the rod did not correlate with the physical spacing of the modulated gain profile that would be required to produce the observed spectral modulation.

In order to investigate further the effect of pump beam quality on the spectrum, the spectrally dispersed Cr:LiSAF laser was pumped at 488 nm with a spatially uniform beam from an argon ion laser. Despite only being able to reach 2.5 mW output power from this spectrally dispersed laser, compared to > 50 mW with the diode pumped laser (due to inappropriate rod coatings, the higher quantum defect in Cr:LiSAF at 488 nm and the thermal damage threshold), we still observed highly modulated spectra. The origin of this structure was not structure in the pump beam and so we attribute it to path dependent loss in the laser crystal due to scattering centres and/or facet/coating irregularities.

The effect of translating the rod horizontally, perpendicular to the pump beam, was to tune the entire spectrum and to 'slide' the spectral modulation through the spectrum. Vertical translations of the rod resulted in variations in the intensity of the spectral peaks and troughs and disappearance and reappearance of particular structures. These observations suggest that it is inhomogeneities in the laser rod (and therefore the gain profile) that are responsible for the spectral modulation. This was further confirmed by an experiment with the diode-pumped broadband laser in which we added a second pump diode, combined using the orthogonal polarization in an attempt to compensate for any troughs in the pump beam profile by 'steering' the more intense peaks of the second pump beam profile into these troughs. We observed that we could only locally increase and narrow the existing peaks in the spectrum, while decreasing the intensity in the troughs, which appeared to remain fixed relative to the horizontal

position of the crystal in the cavity. In terms of the different laser rods, we observed that while the Cr:LiSAF laser generated the highest output power of 105 mW compared to the Cr:LiSGAF laser (as expected due to its higher gain coefficient) there was no notable improvement in the continuity or smoothness of the spectra, suggesting that the density of scattering centres in both crystals was comparable.

5. 3-D imaging using photorefractive holography

To demonstrate its utility for low coherence interferometry and depth-resolved imaging, the broadband Cr:LiSAF spatially dispersed laser was used as the source to achieve depth-resolved 3-D imaging through a liquid scattering medium. The imaging technique employed was photorefractive holography using the experimental set-up represented in Fig. 3, which was similar to that described in [3].

The output from the broadband laser was coupled into a single mode fibre using a $\times 20$ microscope objective with 75% coupling efficiency and provided 45 mW of spatially coherent, broadband incident radiation, which was collimated using a 4.5 mm focal length aspheric lens and used as the source beam for the 3-D imaging experiment. The output spectrum from the fibre was identical to the spectrum of the beam observed directly out of the laser. Fig. 4 shows a typical output spectrum used for this experiment together with its coherence function as recorded using a Michelson interferometer. As the output spectrum from the laser is not Gaussian in shape we observe residual low intensity lobes on

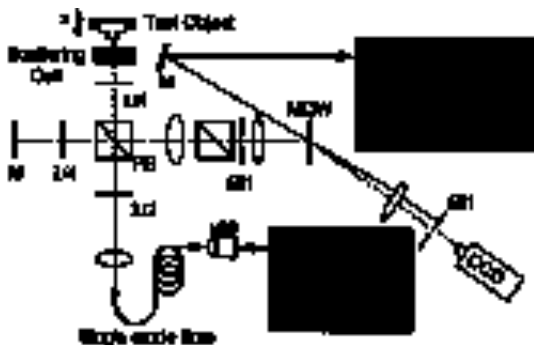
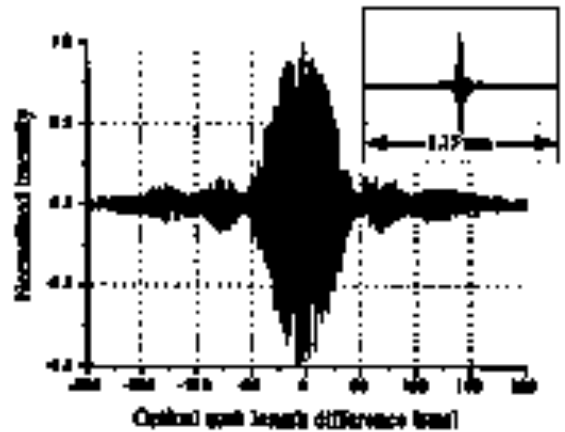


Fig. 3. Schematic of 3-D photorefractive holographic imaging set-up.



(a)



(b)

Fig. 4. (a) Broadband laser spectrum with 13 nm full-width half maximum, corresponding to 45 mW output power from the laser and (b) corresponding interferogram recorded using a Michelson interferometer (with a longer scale insert, in the top right corner).

either side of the main fringes. Ideally these should be minimised by tailoring the spectral profile in order to optimise the depth resolution of the system. We note that these side-lobes would present less of a problem in a microscope imaging system for which the depth resolution would be determined by the convolution of the coherence function and the depth of field of the imaging (objective) lens [6].

Fig. 5 shows depth-resolved images of a 100 μm -stepped 3-dimensional test object consisting of four concentric machined aluminium cylinders. These

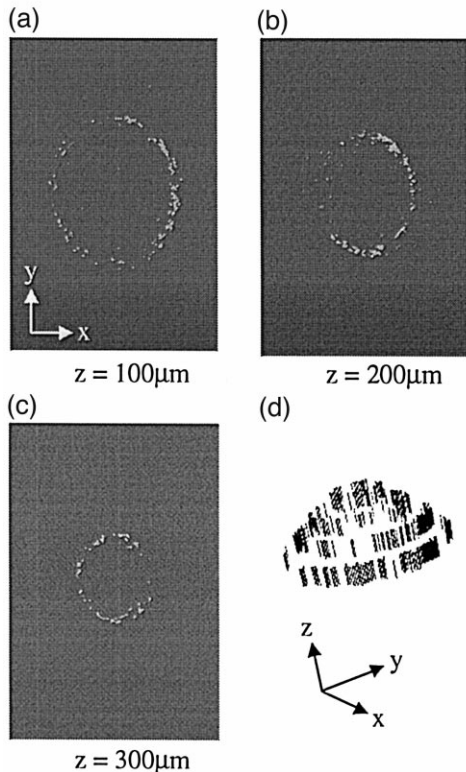


Fig. 5. (a)–(c) holographic images and (d) reconstruction of 3-D test object acquired through ~ 10 mean free paths of liquid scattering medium using spectrally broadened Cr:LiSAF laser.

were imaged through an aqueous suspension of $0.46 \mu\text{m}$ radius polystyrene spheres that exhibited a scattering depth of 9.8 mean free paths in the reflection geometry. As expected from the measured coherence function of the source, the $100\text{-}\mu\text{m}$ steps are easily resolved. The data were acquired in real time and Fig. 5 also shows a computer generated three-dimensional reconstruction of the test object from these experimental data.

6. Conclusions

We have demonstrated a high power, all-solid-state diode-pumped, spectrally broadband and spatially coherent c.w. laser source that takes advantage of the broad gain bandwidths of Cr:LiSAF and Cr:LiSGAF lasers but avoids the complexity of mode locking. This approach inherently counteracts gain

narrowing and should readily scale to higher powers, providing that thermal lensing and other issues associated with high pump powers can be addressed. We note that this technique may be applied to any broadband laser medium. We observed tunable smooth spectra with widths up to $\sim 15 \text{ nm}$ and discontinuous spectra extending up to $\sim 65 \text{ nm}$ wide. We attribute the observed spectral modulation to scattering inhomogeneities in the laser crystal causing path dependent (and therefore wavelength dependent) losses in the cavity. This could potentially be counteracted by eliminating all inhomogeneities in the laser rod or by compensating for them using an element such as an intra-cavity spatial light modulator to ensure a uniform loss for all beamlets. This could also be used to shape the laser spectrum to a desired profile. Using higher pump intensities, e.g. from a diode-array, would allow more flexibility in adjustment of the spatial dispersion while maintaining the laser high above threshold over a broad spectral region, thereby reducing the impact of local scattering centres. These lasers represent a potentially compact, cheap, simple diode-pumped broadband source that can be readily coupled into a fibre for applications such as OCT. We have demonstrated the application of this source to 3-D imaging using depth-resolved photorefractive holography through a scattering medium for the first time.

Acknowledgements

Funding for this research was provided by the UK Engineering and Physical Sciences Research Council (EPSRC) and the Annemarie Schimmel Scholarship Trust.

References

- [1] D. Huang, E.A. Swanson, C.P. Lin, J.S. Schuman, W.G. Stinson, W. Chang, M.R. Hee, T. Flotte, K. Gregory, C.A. Puliafito, J.G. Fujimoto, Optical coherence tomography, *Science* 254 (5035) (1991) 1178–1181.
- [2] N. Abramson, Light-in-flight recording by holography, *Opt. Lett.* 3 (4) (1978) 121–123.
- [3] S.C.W. Hyde, R. Jones, N.P. Barry, J.C. Dainty, P.M.W. French, Sub- $100 \mu\text{m}$ depth-resolved imaging through scattering media in the near infra-red, *Opt. Lett.* 20 (22) (1995) 2330–2332.

- [4] S.V. Chernikov, J.R. Taylor, V.P. Gapontsev, B.E. Bouma, J.G. Fujimoto, A 75-nm, 30-mW superfluorescent ytterbium fibre source operating around 1.06 μm , Technical Digest Series CLEO 11 (1997) 83–84.
- [5] E. Leith, C. Chen, H. Chen, Y. Chen, D. Dilworth, J. Lopez, J. Rudd, P.-C. Sun, J. Valdmanis, G. Vossler, Imaging through scattering media with holography, *J. Soc. Am. A* 9 (7) (1992) 1148–1153.
- [6] E. Beaurepaire, A.C. Boccara, M. Lebec, L. Blanchot, H. Saint-James, Full-field optical coherence microscopy, *Opt. Lett.* 23 (4) (1994) 244–246.
- [7] M. Tziraki, R. Jones, P.M.W. French, D.D. Nolte, M.R. Melloch, Short-coherence photorefractive holography in multiple-quantum-well devices using light-emitting diodes, *Appl. Phys. Lett.* 75 (10) (1999) 1363–1365.
- [8] M.B. Danailov, I.P. Christov, A novel method of ultrabroadband laser generation, *Opt. Commun.* 73 (3) (1989) 235–238.
- [9] M.B. Danailov, I.P. Christov, Amplification of spatially-dispersed ultrabroadband laser pulses, *Opt. Commun.* 77 (5/6) (1990) 397–401.
- [10] M.B. Danailov, I.Y. Milev, Simultaneous multiwavelength operation of Nd:YAG laser, *Appl. Phys. Lett.* 61 (7) (1992) 746–748.
- [11] I.Y. Milev, B.A. Ivanova, M.B. Danailov, S.M. Saltiel, Multi-pulse operation of three-wavelength pulsed Q-switched Nd:Y₃Al₅O₁₂ laser, *Appl. Phys. Lett.* 64 (10) (1994) 1198–1200.
- [12] V.V. Ter-Mikirtychev, Ultrabroadband oscillation of Ti³⁺:sapphire laser, *TOPS Adv. Solid State Lasers* 10 (1997) 177–180.
- [13] J. Faure, J. Itatani, S. Biswal, G. Cheriaux, L.R. Bruner, G.C. Templeton, G. Mourou, A spatially dispersive regenerative amplifier for ultrabroadband pulses, *Opt. Commun.* 159 (1999) 68–73.
- [14] S. Aoshima, H. Itoh, Y. Tsuchiya, Compact geometry for diode-pumped Cr:LiSAF femtosecond laser, *IEEE J. Selected Topics Quantum Electron.* 3 (1) (1997) 95–99.
- [15] M. Ramaswamy-Paye, J.G. Fujimoto, Compact dispersion-compensating geometry for Kerr-lens mode-locked femtosecond lasers, *Opt. Lett.* 19 (21) (1994) 1756–1758.
- [16] D. Kopf, G.J. Spuhler, K.J. Weingarten, U. Keller, Mode-locked laser cavities with a single prism for dispersion compensation, *Appl. Opt.* 35 (6) (1996) 912–915.